Polythiophene nanofilms for sensitive fluorescence detection of viruses in drinking water

Shashwati Wankar, Nicholas W. Turner, Reddithota J. Krupadam

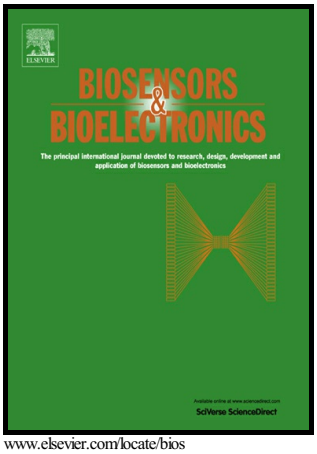

www.elsevier.com/locate/bios

PII: S0956-5663(16)30211-1
DOI: http://dx.doi.org/10.1016/j.bios.2016.03.020
Reference: BIOS8531

To appear in: *Biosensors and Bioelectronic*

Received date: 22 January 2016
Revised date: 7 March 2016
Accepted date: 10 March 2016

Cite this article as: Shashwati Wankar, Nicholas W. Turner and Reddithota J. Krupadam, Polythiophene nanofilms for sensitive fluorescence detection o viruses in drinking water, *Biosensors and Bioelectronic* http://dx.doi.org/10.1016/j.bios.2016.03.020

Polythiophene nanofilms for sensitive fluorescence detection of viruses in drinking water

Shashwati Wankar[a], Nicholas W. Turner[b], Reddithota J. Krupadam[a*]

[a]Environmental Impact and Risk Assessment Division, CSIR-National Environmental Engineering Research Institute, Nehru Marg, Nagpur 440020, India;

[b]Faculty of Science, The Open University, Walton Hall, Milton Keynes, Buckinghamshire MK7 6AA, United Kingdom

[*]Corresponding author: E-mail: rj_krupadam@neeri.res.in; Tel: +91-712-2249 844; Fax: +91-712-2249 896

Abstract

Molecular imprints of the tobacco necrosis virus (TNV) have been formed within polythiophene nanofilms with an approximate thickness of 200 nm. These films have been electrochemically deposited onto conducting Au surfaces. Upon rebinding, the TNV-polythiophene complex changes the fluorescence intensity of the nanofilm. The fluorescence intensity at 410 nm was observed to be proportional to the concentration of viruses in the range of 0.1-10 ng L^{-1} (0.15 – 15 pg) with the lower calculated detection limit of 2.29 ng L^{-1} (3.4 pg). The intensity of the fluorescence emission is not affected by the thickness of the polythiophene film and the nature of TNV specific binding sites. Kinetic data analyses showed that the nanofilm responds to TNV within 2 minutes; and cross-selectivity studies with tobacco mosaic virus (TMV) showed an excellent specificity for the targeted TNV. These binding experiments demonstrate the potential of fluorescence emission for the specific, label free and rapid detection of viruses using nanofilm sensors. Taking into account the lower limit of detection, the fluorescence sensing reported here is reliable, simple to perform, rapid, cost-effective and offers a sensitive analytical method for virus detection in water resources.

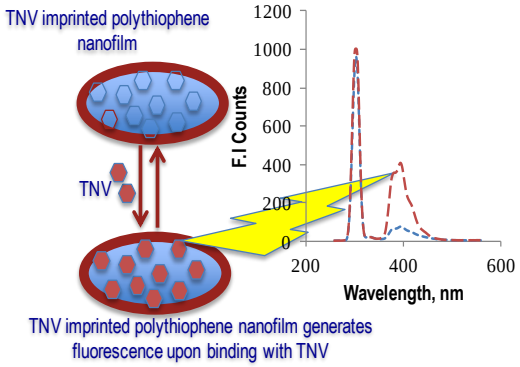

Keywords: Tobacco necrosis virus; Molecular imprinting; Electrochemical sensor; Water sampling; Fluorescence.

1. Introduction

Rapid detection of pathogenic viruses is one of the important tasks for control of waterborne epidemics and homeland security point of view. Access to safe drinking water free of microorganisms and other geogenic pollutants to ~750 million people across the world, as per the estimate of World Health Organization, is still an issue of great public health concern (Yager et al., 2006; Morens et al., 2008). In particular, viral contamination through drinking water causes diseases such as Hepatitis A and E reported major outbreaks in India, China and United States and some other regions (Sinclair et al., 2009). One of the routes to entry of pathogenic human enteric viruses into the public water supply is contamination by sewage. These viruses are prevalent in sewage as the infected patients excrete the viruses in enormous quantities i.e., 10^5 to 10^{11} viral particles per gram of feces (Maunula et al., 2005). Current methods are inefficient to completely destroy viruses. On the other side, detection of viruses in water and other biological fluids is quite difficult due to complicated matrices, sampling concerns and cost. Current practice for virus detection includes polymerase chain reaction (PCR) or cell culture and enzyme-linked immunoassay (Hamza et al., 2011). The ELISA method of analysis is based on the ability of antibodies to specifically recognize the surface of the target virion. However, antibodies are fragile, short-shelf life and high production costs (Dickert et al., 2003; Tai et al., 2006). The maintenance of antibodies is difficult and they are prone to oxidative/microbial degradation and are unusable in harsh environments such as strong acid/alkaline conditions or organic solvents. To potentially counter these

stability issues synthetic receptors called molecularly imprinted polymers (MIPs) have emerged as promising candidates to replace antibodies for sensing and targeted drug delivery systems.

The creation of an artificial molecular recognition site in the robust polymer systems is quite useful in developing highly sensitive detection devices. Molecular imprinting is the leading method to produce such highly target selective polymeric receptors through a fairly generic methodologies (Wulff, 1995; Mosbach and Ramström, 1996; Spivak and Shea, 1999; Piletsky et al, 2001; Sellergren and Allender, 2005). This principle has shown itself to be incredibly flexible in creating specific recognition polymers for small molecules, bioactives, toxins and even larger molecules such as proteins (Hansen, 2007; Verheyen et al., 2011; Whitcombe et al., 2011; Luo et al., 2014; Zhou et al., 2014). The quality of MIPs is decided considering two important criteria: (i) how much more efficient is binding of a given analyte to imprinted (MIP) than to a non-imprinted polymer (NIP) and (ii) how well can we separate two analytes that are only slightly different (e.g., of size and functionality) in spatial patterns of the receptors (Kan et al., 2010). However, it is more difficult to imprint larger targets such as viruses, particularly because their 3D protein structures are flexible and can fluctuate under minimum influence, and MIP technology is still without a standard manufacturing procedure. A number of studies have looked at the problem with varying degrees of success (Tai et al., 2005; Bolisay et al., 2006; Rossi et al., 2007; Krupadam et al., 2009, 2010; Ikawa et al., 2010; Ren and Zare, 2014). Earlier, Dickert's group contributed significantly on the design and development of MIPs for viruses and other microorganisms (Dickert et al., 2004; Hayden et al., 2006; Jenik et al., 2009; Schirhagal et al., 2010). Human rhino virus 14 imprinted MIP nanoparticles formulated with poly(vinylpyrrolidone-*co*-methacrylic acid) and cross-

linked with *N*,*N*'-(1,2-dihydroxyethylene)-bisacrylamide (DHEBA) was immobilized on a 10 MHz quartz crystal microbalance (QCM) and these pronounced good sensor responses. Wang et al. (2010) reported potentiometric sensors based on surface molecular imprinting for detection of poliovirus; however, the reported lower detection limit of the method 4000 virons mL^{-1} which is quite on higher side. One of the reasons for low sensitivity of sensors would be due to difficulty in migration of high molecular weight viron particles onto the sensing material which is imprinted with specific virus. Sykora et al. (2015) described a synthetic strategy to produce organic/inorganic nanoparticulate hybrids that recognize non-enveloped icosahedral viruses in water at concentrations down to the picomolar range. The reported method, which is based on surface imprinting using silica nanoparticles that act as a carrier material and organosilanes serving as biomimetic building blocks, goes beyond simple shape imprinting. Bai and Spivak (2014) reported a new "double imprinting" method whereby a virus-bioimprinted hydrogel is further micromolded into a diffraction grating sensor by using imprint-lithography techniques to give a "Molecularly Imprinted Polymer Gel Laser Diffraction Sensor" (MIP-GLaDiS). A simple laser transmission apparatus was used to measure diffraction and the system can read by the naked eye to detect the Apples Stem Pitting Virus (ASPV) at concentrations as low as 10 ng mL^{-1}, thus setting the limit of detection of these hydrogels as low as other antigen-binding methods such as ELISA or fluorescence-tag systems. Altintas et al (2015a) developed very effective MIP based surface plasmon resonance (SPR) biosensor for detection of bacteriophage MS2. A high affinity between the artificial ligand and the target bacteriophage MS2 was found, and a regenerative MIP-based virus detection assay was successfully developed using a new surface plasmon resonance (SPR)-biosensor which provides an alternative technology

for the specific detection and removal of waterborne viruses. The same group also developed adenovirus sensors using MIPs and achieved the limit of detection as 0.02 pM (Altintas et al., 2015b). As an alternative to MIP receptors, direct and sandwich assays were developed for adenovirus quantification using natural antibodies. The detection limit of direct and sandwich assays were found as 0.3 pM and 0.008 pM, respectively. The performance of the new method of sensing in this study is compared with methods reported in the literature (Support information, SI-Table 1).

In this study we have elected to use a polymer thinfilm as a sensory material of a single functional and cross-linking monomer terthiophene. The use of a single electropolymerised monomer reduces the risk of any external disrupting the template-monomer complex, hence affecting the imprinting process. By using a thin film the template loading into the film is closer to the interface and thus less template analyte need to be rebinded and detected. The so-called 2D vs 3D effect is true for all large molecules as discussed in terms of proteins here (Turner et al., 2006). The deposition of a thin film *via* electropolymerisation is controllable, reproducible and cost effective. Furthermore, the material used is stable in water and proved able to detect the viruses from water which is a positive step towards practical use, as demonstrated in the Altintas (2015 a,b).

In this work the tobacco necrosis virus (TNV) was imprinted into a thin polythiophene film of thickness less than 200 nm. The inherent robustness, small size (~20 nm) and spherical shape of the TNV (Horne, 2014) makes it an ideal candidate for model imprinting experiments in polymers. The film was supported on a gold coated conducting gold surface (CGS) which was used as the working electrode in the three-electrode electrochemical cell setup. The electrochemical technique reported in

this study is rapid, sensitive and quite simple compared with surface imprinting methods such as stamping and spin coating. Imprinting of interesting targets such as viruses using electrodeposition on cost-effective conducting glass surface is capable of generating uniform thickness nanofilms in the range of (20-500 nm). Analysis was by fluorescent interrogation of the film is one of the sensitive approach.

2. Materials and Methods

Solvents (acetonitrile, dicholoromethane, ethanol) of HPLC/Spectroscopic grade were purchased from Fisher (Pittsburg, PA, USA). Tobacco Necrosis Virus (TNV) and Tobacco Mossaic Virus (TMV) were purchased from LoeweBiochemica GmbH, Sauerlach, Germanyand stored at -20° C until use. Tetrabutylammoniumhexa fluorophosphate (TBAH) and terthiophene was purchased from Merck (Kenilworth, MA, USA)and used as found.

2.1. Preparation of MIP nanofilm by electrodeposition method

Prior to electropolymerization, the CGS was cleaned in piranha solution for 60 s [1:3 (v/v) H_2O_2/H_2SO_4] and then subjected to plasma cleaning using a March Plasmod GCM 200 (Concord, CA, USA) for 150 s at 10 W with an argon gas purge.

2 mL of 1 mM tobacco necrosis virus was added to 18 mL of 4 mM terthiophene in acetonitrile with 0.1 M tetrabutylammoniumhexafluorophosphate (TABH, 750 mg in 20 mL) to form a working solution. The solutions were stored at 4°C for about 10 h before electropolymerization; and this time allow to form complex between monomer and template.

20 mL of the solution was then used to coat a prior prepared CGS of 1.50 cm^2 by voltammetric cycling in acetonitrile. The voltammetric cycling was conducted using 20 consecutive cycles in the potential range from 0 to 1.2 V at 150 mV s^{-1}. Cyclic voltammetry (CV) was performed on an Power Lab System potentiostat

(Milano, Italy) containing 3-electrode cell with platinum wire as the counter electrode; Ag/AgCl wire as the reference electrode and the CGS as the working electrode. The cell temperature was set at 20°C. The TBAH solution of 0.1 M was used throughout the study to characterize the electrochemical response on the both MIP and non-imprinted polymer (NIP) coated electrodes.

After electrodeposition, the films were washed with acetonitrile to remove excess monomer from the polymer film. Finally, the template was removed from electropolymerized MIP by dipping in acetonitrile, dichloromethane and ethanol solvents for 15 minutes each.

Non-imprinted polythiophene films, to be used as controls, were prepared in a similar manner using the same procedure without the TNV in the working solution.

2.2. Characterization of Polymer Nanofilms

The surface area and pore parameters of the polymer films were measured using N_2 porosimeter (JEOL JSM-6400, Peabody, USA). A small portion of polymer film was degassed at 70°C under nitrogen flow for approximately 6 h prior to measurement. The nitrogen adsorption/desorption data were recorded at the liquid nitrogen temperature (77 K). The specific surface area was calculated using the Brunauer–Emmett–Teller (BET) equation. The mesopore size distributions were determined by Barrett–Joyner–Halenda (BJH) method, while those of the micropore were determined by micropore analysis method. All reported data represent the results of three to five concordant experiments, with standard deviation below 5%.

Ellipsometry was used to measure the thickness of the electropolymerized film using the Multiskop ellipsometer (Optrel GmbH, Germany) equipped with a 632.8 nm laser. Contact angle measurements were done on a CAM 200 optical contact angle meter (KSV Instruments Ltd.).

AFM measurements were performed using a Flex AFM from Nanosurf (FlexAFM, Liestal, Switzerland) using topping mode with scanning rate between 1 and 1.5 lines s^{-1}. Commercially available tapping mode tips (TAP300-10, Silicon AFM probes, Tap 300, Ted Pella, Inc.) were used on cantilevers with a resonant frequency in the range of 290-410 kHz. All AFM micrographs were filtered and analyzed using the Easyscan Software.

2.3 TNV Detection system

Fluorescence intensity measurements were performed on a fluorescence spectrometer (Hitachi F-4500, Tokyo, Japan). The instrument includes a light source (75 W xenon Lamp), a model 101M monochromator and a model 814 detector. Fluorescence of the samples were recorded using a fixed excitation wavelength (260 nm), and the intensities of fluorescence emission 410 nm were used for quantification of viruses.

The binding and molecular recognition properties of the polythiophene nanofilm for the targeted TNV were evaluated by equilibrium binding analysis. The gold surface coated with MIP or NIP was fixed in a holder; which is connected to syringe pump to inject TNV solution (1 ng L^{-1}; 1.5 pg) with the flow rate of 50 µL min^{-1}. The drain from the system was collected at regular intervals and the solutions were analyzed for TNV concentration using fluorescence spectrometer (λ_{Ex}, 290 nm; λ_{Em}, 410 nm). The percentage of TNV binding to any polymer was calculated using a subtraction method from the original injection concentration, against a pre-generated calibration curve obtained from external TNV standards.

Throughout each experiment, the film was monitored at one minute intervals for fluorescence emission. A pulse measurement method was decided upon to limit

risk of bleaching. The optimum response time (<2 min) was determined by measuring residual TNV concentration in solution at different flow times.

Three repeated measurements were performed for every sample, and the mean of the concentration was used to plot subsequent data.

The sensing of TNV using the fabricated MIP film was performed on the fluorescence spectrometer with a flow channel set-up. During sensing, the fluorescence was set to automated injection of Milli-Q water (pH, 7.0±0.3) for 120 s followed by sample injection (1 mL) for 30 s, and then rinsing of the MIP film with the background solution for 60 s. The fluorescence response due to the binding of TNV and TMV were compared and plotted after change in intensity. All the fluorescence measurements of adsorption capacity and kinetic curves were normalized to zero and plotted in OriginLab (ver. 7)

3. Results and Discussion

The electrodeposition of the polymer films proved to be relatively straightforward, which provided with reproducible and fairly uniform layers. In this respect it is quicker than a stamping procedure previously reported (Jiang et al., 2010). Using a single functional monomer providing recognition and cross-linking stability is favourable for these types of imprinted films.

The composition of MIP and NIP solutions used in cyclic voltammeter and the corresponding surface properties of the polymer films are given in Table 1. The cyclic voltagrams (CV) of MIP and NIP films deposition depict the typical redox peak of polythiophene with an onset potential at 0.62 V and 0.78 V for MIP and NIP, respectively (Support Information, SI-Fig.1a,b). The anodic peak beyond 1.06 V in the first CV scan has been reported to be due to the formation of the terthiophene radical cation, which is achieved by losing an electron in the neutral monomer species

(Pernites et al., 2011). Then, during the reverse scan (reduction), the radical cation is expected to couple with another charged species to form a dimer. In the second CV cycle, a new oxidation peak appears at a relatively lower potential (between 0.6 and 1.0 V), which is related to the formation of a more stable dication (bipolaron) with extended Π-conjugation that is easily oxidized compared to the radical cation. Upon succeeding CV cycles until 20^{th}, the current increases at this redox peak (between 0.6 and 1.0 V), indicating the formation of oligomers and polymer as a result of the further cross-linking between the terthiophene units. For NIP film, the similar trend as MIP film was followed; however, the peak intensities and potential are higher compared with the MIP film evidences TNV deposition imprinting on MIP film. The overall electrodeposition of the polythiophene film onto the CGS is evidenced by the net increase in the mass (0.31±0.05 mg) after 20 CV cycles as measured gravimetrically by analytical five point microbalance and the clear deposition of materials visible to the naked eye (Photographs of CGS are given in SI-Fig.2). The thickness of TNV imprinted polymer film was 200±10 nm which is slightly thinner than the NIP film. It is interesting note that by increasing the number of cycles, even though increase in the thickness of the polymer film, there is no considerable change in polymer surface properties such as surface area, pore volume and pore diameter. However, noticeable increase in mass of the polymer deposition was found with increasing number of cycles (Table 2). Also, the thickness of MIP film is slightly less than the NIP film for a given number of cycles. The film with thickness 200±10 nm was used for binding experiments. Such a thin polymer surface imprinted with virus allowed for ease of access for analyte virus to the binding pockets, suggesting that this method may improve the sensitivity of the sensor (Pernites et al., 2012).

The morphology of the MIP and NIP was viewed by atomic force microscope (AFM). The existence of specific cavities in the MIP films and thus evidence of TNV imprinting; while the NIP without specific cavities in the film (Support Information, SI-Fig.3). The size of imprinted cavities is ~20 nm and spherical in shape represent the morphology of TNV. AFM images of the TNV imprints and non-imprints show the imprints correctly reproduce the geometrical features of the virus-TNV. The imprinting effect changes the morphology of the polymer (Turner et al., 2009). The templating of TNV on the polymer surface improved the surface area from 126 $m^2 g^{-1}$ to 189 $m^2 g^{-1}$ and the pore volume of MIP is 0.079 cm^3/g which is slightly higher than the NIP (Table 2). The SEM micrographs of TNV imprinted polymer and TMV imprinted polymer clearly shows the copies of viruses formed on the polythiophene nanofilm (Support information, SI. Fig.4). A small portion of MIP film analysis reveals that recognition cannot be based only on geometry, as the imprinted cavities about 20 nm deep and this is strongly indicative of two different interaction processes leading to the binding event; obviously there are patterns in the 10-100 nm range depicting the geometrical features of the analytes. The AFM micrograph of TMV imprinted polymer shows formation of cylindrical structures in the polythiophene film (Support information, SI.Fig.5). These cavities additionally have to contain structures on the molecular level that are responsible for the interaction network between the TNV and the polythiophene nanofilm.

The binding of TNV on the MIP and NIP nanofilms were conducted in a self-designed flow reactor depicted in Support Information, SI-Fig.6. The TNV solution of concentration 1.0 ng L^{-1} (1.5 pg) was passed through the micro-column set-up which is equipped with syringe pump system and the drain after passing through the CGS surface was collected at drain in the regular intervals. The concentration of TNV in

the drain samples were analyzed using fluorescence. In the similar way, by varying different concentrations (0.5, 1, 2, 3, 4, 5, 7, and 10 ng L^{-1}) of TNV solution the binding capacity of the imprinted polymer film is determined. A calibration curve for different TNV concentrations in aqueous solutions is monitored and unknown concentration of TNV from the CGS drain is determined from calibration graph. The drain of CGS was analyzed with fluorescence spectrometer with excitation wavelength (λ_{ex}, 270 nm) and emission wavelength (λ_{em}, 410 nm) is monitored. The binding capacity of TNV on the MIP and NIP was measured by monitoring change in fluorescence intensity (λ_{em}, 410 nm) at emission wavelength. The working range of TNV solution was 0.2 - 10.0 ng L^{-1} (0.3 – 15 pg) and the binding capacity of the films are depicted in Fig.1a. It can be seen that the dynamic binding capacity of TNV almost linearly increased when its concentration was less than 1.0 ng L^{-1} (1.5 pg). The same binding capacity was observed when the TNV concentration was higher than 1.0 ng L^{-1}.The binding affinity of MIP for both TNV and TMV has been computed from the following equation (1) via dissociation constants.

$$B = B_{max}c/(k_d+c) \quad \text{--------- Eq. (1)}$$

where c is the concentration of TNV/TMV and B is the fraction of TNV specific sites (Tai et al., 2005). The specific TNV sites are related to the fluorescence intensity by:

$$B = F.I/MW \quad \text{-------- Eq. (2)}$$

where F.I is the fluorescence intensity of CGS and MW is the molecular weight of TNV/TMV. The molecular weight of TNV and TMV considered for calculation are $4.08x10^7$ and $2.80x10^5$ D, respectively (Johnson and Brown, 1992). It was found that the MIP had a k_d value of 30 nM for TNV and 10 nM for TNV and TMV, respectively. The smaller size of TNV would possibly easy to dissociate from polymer to create better imprinting sites than the relatively bigger TMV. The k_d

values show that TNV is more inclined to bind to the MIP due to TNV copies formed inthe polymer with appropriate surface charge and functionality.

The breakthrough capacity curve for TNV was observed to be a symmetrical S-shape which is due to the non-equilibrium condition developed when the TNV solution flow faster than the diffusion rate of TNV onto the MIP film (Fig.1b). The curve is steep at the breakthrough point. The TNV breakthrough column started after 5 mL, when the flow rate, 50 μL min^{-1} the concentration of TNV in the effluent was below 0.03 ng L^{-1} (30 times less the initial TNV flow concentration, 1.0 ng L^{-1} (absolute mass, 1.5 pg). The course of the breakthrough curved indicated that TNV effectively trapped in the virus imprinted sites of the MIP film. It appears that mass transport of the TNV binding to the binding sites may limit the effective capacity observed at these flow rates. These experimental results showed that the adsorption in this system is a rapid kinetic process. The time for the fluorescence response to reach a stable peak height with each incremental addition of the analyte into the micro-column was observed to be between 0.2 and14 minutes. A complete curve typically requires 15 minutes to obtain. This result suggests that a non-linear adsorption isotherm occurred for adsorption of TNV on the MIP films, which may be caused from the specific TNV imprinted sites on the MIP film and they are absent in NIP film. The NIP film has almost straight line with quite low adsorption of TNV.

The MIP film response of fluorescence to incremental concentration of TNV was recorded. Intensity of fluorescence peak at λ_{em}, 410 nm was quite high for 10 ng $L^{-1}$of TNV solution and it reaches its plateau at about 0.4 ng L^{-1}(0.6 pg). For the selectivity studies, rod-shaped and quite bigger virus TMV was used and it was found that MIP nanofilm is selective towards TNV (Fig.2). The specificity of the fluorescence response was tested using the tobacco mosaic virus (TMV) in aqueous

solution showed no fluorescence peak at 410 nm at 10 ng L^{-1} (15 pg) identical to the TNV. Non-imprinted polymer film when contacted with TNV, the fluorescence intensity was unchanged. The specificity of the MIP depends on the degree of complementary cavities to the target produced during the molecular imprinting, whereas nonspecific interactions would be due to chemical functionality of the target and the MIP. The sensor response of MIP and NIP nanofilms towards the target TNV solution of 1 ng L^{-1} (1.5 pg) TNV, clearly demonstrates the effect of imprinting. Evidently, the pores generated by the imprinting process lead to interaction sites that are reoccupied when exposed to TNV, leading to fully reversible fluorescence emission. Thus, the imprinting of TNV on polythiophene films leads to excellent selectivity between different virus types. The extraction of bound TNV from polythiophene film provides very important information about the nature of binding responsible for molecular recognition. The extraction of virus from MIP film was quantified by the intensity of fluorescence in solution water the wash with acetonitrile was performed. The per cent template removed from acetonitrile wash was highest (87%) compared with methanol (59%), IM NaOH (66%) and 5M urea (62%). This is an indication that the polythiophene surface was associated with the virus through its thiophene groups and not by just surrounding the virus (TNV) template.

The concentrations considered for the measurement with CGS coated MIP nanofilm are in the range 0.1 - 100 ng L^{-1} (0.15 – 15 pg) in water (Fig.3). These showed a distinct relationship between the fluorescence signal and the TNV concentration. The linear fit through the data points gives a correlation coefficient of 0.98 represents that the TNV concentration predictions given in the calibrated MIP nanofilm fluorescence sensor. From these results, and given the signal-to-noise ratio at λ_{em}410 nm that was observed an effective LOD of 2.29 ng L^{-1} (3.43 pg) was

calculated (Table 3). High sensitivity, short-time response, stability in aqueous solutions, and the prospect to develop the cost-effective sensor as a robust handheld device, it is anticipated that the MIP nanofilm fluorescence virus sensor is a potential candidate for monitoring of viruses in aqueous solutions such as drinking water.

Conclusions

A sensitive, rapid and reusable MIP nanofilm based fluorescence sensor is reported for virus detection in drinking water. Tobacco necrosis virus is chosen based on its small size and spherical shape (morphologically same as many viruses causing water-borne diseases) as the model virus. The following are important conclusions of the study:

i. Polythiophene nanofilms of thickness 100-500 nm were produced by electropolymerization; and the method proposed has the merits such as simple, rapid and reproducible thickness of the polymer films, reusability and cost-effective.

ii. Using a single functional monomer providing recognition and cross-linking stability is favourable for large templates in 2D format. The larger templates such as viruses and microorganisms, with high cross-linking densities hinder mass transfer of the template, leading to slow template removal and rebinding kinetics, which restricts sensing applications.

iii. Polythiophene nanofilm imprinted with TNV showed high sensitivity for detection of viruses in aqueous solutions in the concentration range between 1 - 100 ng L^{-1} and the lowest detection limit of 2.29 ng L^{-1} was achieved by measurable fluorescence emission at 410 nm.

Acknowledgment

We appreciate financial support from Council of Scientific & Industrial Research (CSIR), New Delhi, India under Clean Water Project (Grant No. WM 2A.3.2; Pathogenic Virus Sensor Development)

References

Altintas, Z., Gittens, M., Guerreiro, A., Thompson, K. A., Walker, J., Piletsky, S.A., Tothill, I.E., 2015a. Anal. Chem., 87, 6801-6807.

Altintas, Z., Pocock, J., Thompson, K.A., Tothill, I.E., 2015b. Biosens. Bioelectron., 74, 996-1004.

Bai, W., Spivak, D.A., 2014. Angew. Chem. Int. Ed., 53, 2095-2098.

Bolisay, L.D., Culver, J.N., Kofinas, P., 2006. Biomater. 27, 4165-4168.

Dickert, F.L., Liberzeit, P.A., Hayden, O. 2003. Anal. Bioanal. Chem. 377, 540-549.

Dickert, F.L., Lieberzeit, P.A., Miarecka, S.G., Mann, K.J., Hayden, O., Plafinger, C. 2004. Biosens. Bioelectron. 20, 1040–1044.

Hansen, D.E., 2007. Biomater. 28, 4178-4191.

Hayden, O., Bindeus, R., Haderspöck, C., Mann, K.J., Wirl, B., Dickert, F.L., 2003, Sens. Actuators B: Chem. 91, 316-319.

Horne, R.W., 2014. Virus structure. Academic Press. Waltham MA, USA.

Ikawa, T., et al., 2010. Langmuir, 26, 12673-12679.

Jenik, M., Schirhagl, R., Schirk, C, Hayden, O., Liberzeit, P., Blass, D., Pual, G., Dickert, F.L., 2009. Anal. Chem., 81, 5320-5326.

Jiang, G., Ponnapati, R., Pernites, R., Felipe, M.J., Advincula, R.C., 2010. Macromol., 43, 10262-10274.

Johnson, P. , W. Brown. 1992. An investigation of rigid rod-like particles in dilute solution. In Laser Light Scattering in Biochemistry. S. E. Harding, D. B. Sattelle, and V. A. Bloomfield, Editors. Royal Society of Chemistry, Cambridge.161-183.

Krupadam, R.J., Bhagat, B., Khan, M.S., 2009. J. Nanosci. Nanotechnol. 9, 5441-5447.

Krupadam, R.J., Khan, M.S., Wate, S.R., 2010. Water Res. 44, 681-688.

Maunula, L., Miettinent, I.T., Bonsdorff, C.H., 2005. Emerg. Infect. Dis., 11, 1716-1721.

Morens, D.M., Folkers, G.K., Fauci, A.S., 2008. Lancet Infect. Dis., 8, 710-719.

Mosbach, K., Ramström, O., 1996. Nat. Biotechnol., 14, 163-170.

Pernites, R., Ponnapati, R., Felipe, M.J., Advincula, R.C., 2011. Biosens. Bioelectron., 26, 2766-2771.

Pernites, R.B., Venkata, S.K., Tiu, B.D.B., Yago, A.C.C., Advincula, R.C., 2012. Small, 8, 1669-1674.

Piletksy, S.A., Piletska, E.V., Bossi, A., Karim, K., Lowe, P., Turner, A.P.F., 2001. Biosens. Bioelectron., 16, 701-707.

Ren, K., Zare, R.N., 2012. ACS Nano., 6, 4313-4318.

Rossi, A.M., Wang, L., Reipa, V., Murphy, T.E., 2007. Biosens. Bioelectron., 23, 41-745.

Luo, S.C., Sivashanmugan, K., Liao, J.D., Yao, C.K., Peng, H.C., 2014. Biosens. Bioelectron., 61, 232-240.

Schirhagal, R., Lieberzeit, L.A., Dickert, F.L., 2010. Adv. Mater., 22, 2078-2081.

Sellergren, B., Allender, C.J., 2005. Adv. Drug. Deliv. Rev., 57, 1733-1741.

Sinclair, R.G., Jones, E.L., Gerba, C.P., 2009. J. Appl. Microbiol., 107, 1769-1780.

Spivak, D.A., Shea, K.J., 1999. J. Org. Chem., 64, 4627-4634.

Sykora, S., Cumbo, A., Belliot, G., Pothier, P., Arnal, C., Dudal, Y., Corvini, P.F.-X., Shahgaldian, P., 2015. Chem. Commun., 51, 2256-2258.

Tai, D.F., Lin, C.Y., Wu, T.Z., Chen, L.K., 2005. Anal. Chem., 77, 5140-5143.

Tai, D.F., Lin, C.Y., Wu, T.Z., Huang, J.H., Shu, P.Y., 2006. Clin. Chem., 52, 1486-1491.

Turner, N.W., Holmes, N., Brisbane, C., McGeachie, A. B., Bowyer, M. C., McCluskey, A., Holdsworth, C.I., 2009. Soft Matter, 5, 3663-3671.

Turner, N.W., Jeans, C.W., Brain, K.R., Allender, C.J., Hlady, V., Britt, D.W., 2006. Biotechnol. Prog., 22, 1474-1489.

Verheyen, E, Schillemans, J.P., van Wijk, M., Demeniex, M.A., Hennink, W.E., van Nostrum, C.F., 2011. Biomater. 32, 3008-3020.

Wang, Y., Zhang, Z., Jain, V., Yi, J., Mueller, S., Sokolov, J., Liu, Z., Levon, K., Rigas, B., Rafailovich, M.H., 2010. Sens. Actuators B: Chem., 146, 381-387.

Whitcombe, M.J., Chianella, I., Larcombe, L., Piletsky, S.A., Noble, J., Porter, R., Horgan, A., 2011., Chem. Soc. Rev., 40, 1547-1571.

Wulff, G., 1995. Angew. Chem. Int. Ed., 34, 1812-1832.

Yager, P., Edwards, T., Fu. E., Helton, K., Nelson, K., Tam., M.R., Beigl, B.H., 2006. Nature, 442, 412-418.

Zhou, J., Gan, N., Li, T., Hu, F., Li, X., Wang, L., Zheng, L., 2014. Biosens. Bioelectron. 54, 199-206.

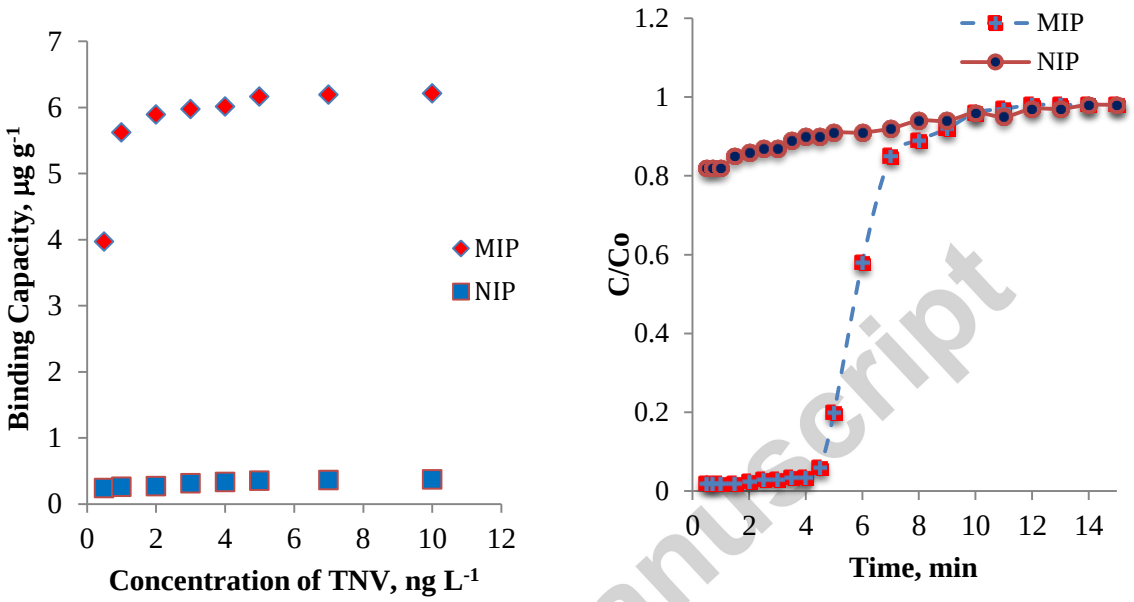

Fig.1. (a) Binding capacity of MIP and NIP for TNV at different initial concentration of TNV and drain collected from outlet of the micro-column at every 1 min. Coefficient of variation (CV) of the measurement is 4.72%. (b) Breakthrough curve of TNV adsorption onto polythiophene thin-film in a micro-column. CV of the measurement is 4.29%. Flow rate, 50 µL min^{-1}; concentration 1 ng L^{-1} (absolute mass, 1.5 pg); Temperature, 25°C. Number of measurements carried out for each experiment are *(n=5)*.

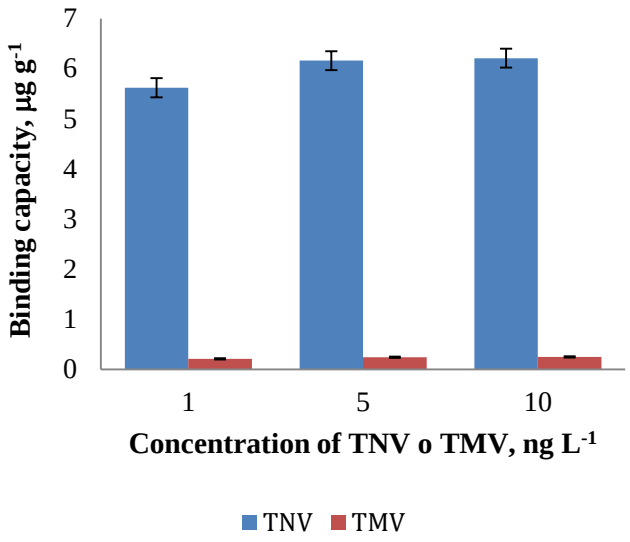

Fig.2. TNV and TMV binding to TNV-imprinted polymer. CV = 4.97%. Binding conditions followed for the experiment are, initial concentration of TNV or TMV, 1 ng L^{-1} (1.5 pg) ; polymer surface area, 1.5 cm^2; flow rate, 50 µLmin^{-1}. Number of measurements carried out for each experiment are 3 *(n=3)*.

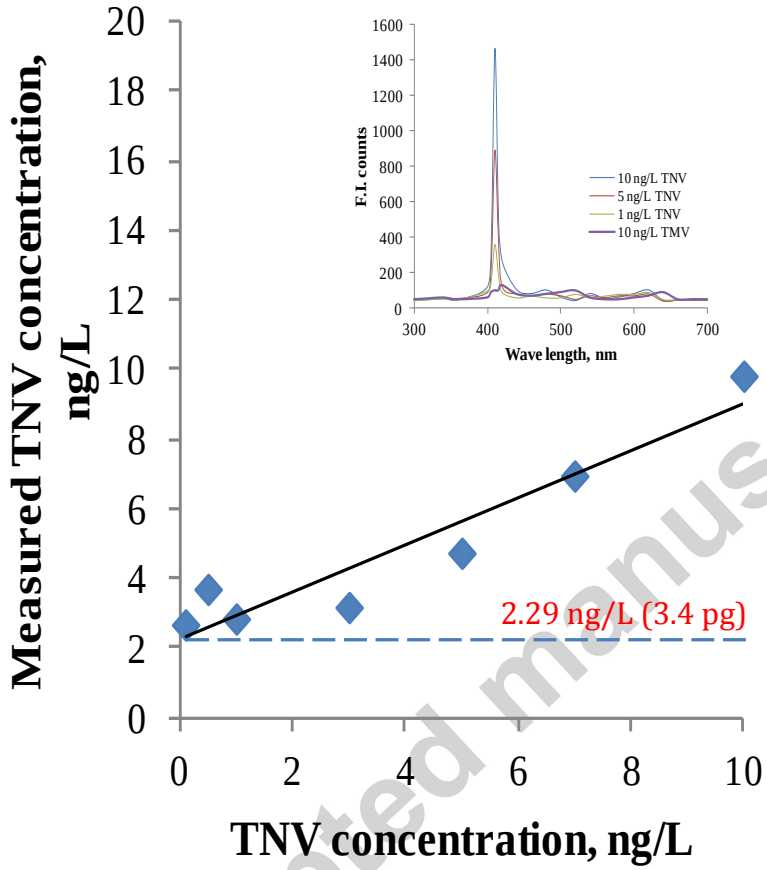

Fig.3. MIP nanofilm fluorescence response to TNV. Lowest detection concentration of TNV in aqueous solution is 2.29 ng L^{-1} (absolute mass, 3.4 pg). Inset: fluorescence spectra recorded for TNV at different concentration in aqueous solution. TMV is not showing any peak at λ_{em}, 410 nm.

Table 1. Composition and surface properties of TNV imprinted and non-imprinted nanofilm

Polymer nanofilm	**Composition**				**Surface properties**		
	Template, TNV(μg)	Monomer, Terthiophene, (g)	Electrolyte, TBAH (mg)	Solvent, Acetonitrile (mL)	SA_{BET}, m^2g^{-1}	APV, cm^3g^{-1}	APD, nm
MIP	50±5	4.98	750	20	189	0.079	25±5
NIP	-	4.98	750	20	126	0.053	93±10

MIP, molecularly imprinted polymer; NIP, non-imprinted polymer; TNV, Tobacco necrosis virus; TBAH, tetrabutylammoniumhexafluorophosphate; SA_{BET}, BET Surface area; APV, Average pore volume; APD, Average pore diameter.

Table 2. Polymer thickness and surface properties are the function of number of cycles

	MIP			NIP		
Number of cycles	10	20	30	10	20	30
Film thickness, nm	110	200	350	140	300	410
Mass of the film, mg	0.18	0.31	0.46	0.23	0.39	0.55
Surface Area,m^2g^{-1}	191	189	183	133	126	130
Pore volume, cm^3g^{-1}	0.081	0.079	0.076	0.051	0.053	0.056
Average pore diameter, nm	23	25	27	87	93	96

Electropolymerization was performed in a 3-electrode cell and the 3-electrode system of the cell is Ag/AgCl (reference electrode); Pt (counter electrode) and CGS (working electrode). The potential range applied was 0-1.2 V with scan rate of 150 mV/s for 20 cycles. Number of cycles were changed in the potentiostat for 10 and 30. The working solution consists of 2 mL of 1 mM tobacco necrosis virus and 18 mL of 4 mM terthiophene in acetonitrile with 0.1 M tetrabutylammonium hexafluorophosphate (TABH, ~750 mg in 20 mL). The mass of the film was measured gravimetrically in an analytical balance while the film thickness was measured using elipsometer with light source as the laser. The surface properties were measured in JEOL JSM-6400.

Table 3. Fluorescence sensing performance of MIP nanofilm for TNV in water

Concentration of TNV, ng/L (pg)		**CV(%)**	**Bias(%)**	**LOD, ng/L (pg)**
Added	**Measured**			
0.1 (0.15)	2.69 (4.03)	7	-6	2.35 (3.52)
0.5 (0.75)	3.71 (5.56)	11	-11	2.49 (3.74)
1 (1.50)	2.86 (4.29)	9	-4	2.29 (3.43)
3 (4.50)	3.19 (4.78)	4	1	2.31 (3.46)
5 (7.50)	4.75 (7.36)	3	2	2.28 (3.42)
7(10.5)	6.97 (10.43)	6	2	2.29 (3.43)
10 (15.0)	5.84 (8.76)	5	1	2.28 (3.42)

Fluorescence emission intensity was measured at 410 nm with standard TNV virus solutions (1.0-20.0 ng L^{-1}) prepared in Milli-Q water. A standard addition plot was constructed and the linear regression was performed on the data points. The slope is the regression corrections to the lowest possible sensing

concentration. CV(%) = (SD/Mean)x100; Bias (%) = [(measured concentration - spiked concentration) /spiked concentration]x100. LOD = Three times the standard deviation calculated at the spiked level considered (RSD, n=3)

Highlights

- Molecular imprints of the tobacco necrosis virus (TNV) within polythiophene nanofilms
- Single functional monomer provided favorable recognition and cross-linking stability for imprinted films
- TNV-polythiophene changes the fluorescence intensity of the nanofilm upon binding with TNV
- Sensitive range of TNV concentration is 0.1-10 ng L^{-1} with lower detection limit of 2.29 ng L^{-1}
- Fluorescence emission intensity is not affected by the thickness of the polythiophene film
- Nanofilm responds to TNV within 2 minutes and an excellent specificity for the targeted TNV